

Soda Feldspar as a Natural Mineral Adsorbent for Methyl Violet Removal from Aqueous Solutions: Equilibrium, Kinetic, and Thermodynamic Studies

Madhusudhana Reddy. Mule^{1*}, G. V. S. Sarma², K.V. Ramesh² and K. Sarath Chandra³

¹Department of Chemical Engineering, RGUKT Nuzvid, Nuzvid-521202, India.

(Email: msreddy.mule@rguktn.ac.in)

²Department of Chemical Engineering, Andhra University College of Engineering (A), Visakhapatnam-530003, India

³SCRACS(OFC) Pvt. Ltd., Buchireddypalem-524305, India.

Abstract

Soda feldspar, a naturally abundant and inexpensive mineral, was investigated as an adsorbent for the removal of methyl violet (MV) dye from aqueous solutions. Batch adsorption experiments were carried out to examine the influence of key operating parameters, including contact time, solution pH, and adsorbent dosage. The adsorption performance was found to depend strongly on these parameters, with optimum conditions observed at a contact time of 90 min, pH 7, and adsorbent dosage of 20 g L⁻¹ with a maximum dye removal efficiency of 95.4%. The adsorption kinetics were evaluated using pseudo-first-order and pseudo-second-order models. Among them, the pseudo-second-order model showed a much better correlation with the experimental data ($R^2 = 0.99$). Equilibrium data were analysed using Langmuir, Freundlich, Temkin, Redlich–Peterson, and Dubinin–Radushkevich isotherm models. The Langmuir model provided the best fit ($R^2 = 0.99$) with a maximum adsorption capacity of 3.91 mg g⁻¹, suggesting predominantly monolayer adsorption on the adsorbent surface. Thermodynamic analysis revealed negative Gibbs free energy values confirming the spontaneous nature of adsorption, while the positive enthalpy change ($\Delta H^\circ = 11.521 \text{ kJ mol}^{-1}$) indicated that the process is endothermic. Overall, the results demonstrate that soda feldspar can serve as a promising, environmentally friendly, and cost-effective adsorbent for the treatment of dye-contaminated wastewater.

Keywords: Soda feldspar; Methyl violet; Adsorption; Adsorption kinetics; Adsorption isotherms; Thermodynamic studies; Wastewater treatment; Dye removal.

1. INTRODUCTION

Water is a fundamental resource for human survival, economic development, and ecosystem sustainability. But, due to increasing industrialization and urbanization large quantities of untreated wastewater is discharged into natural water bodies, causing serious environmental concerns. Among various industrial pollutants, synthetic dyes are considered to be one of the

most significant contaminants due to their high visibility, persistence, and toxic nature[1],[2].

Textile effluents contain significant quantities of dyes and chemicals which lead to heavy water pollution[3]. Over 100,000 commercial dyes are available globally and more than 700,000 tons of dyes are produced every year[4],[5]. The release of these dye-containing effluents into aquatic systems reduces light

penetration, inhibits photosynthesis, and disturbs aquatic ecosystems[6],[7].

Among the various classes of dyes, methyl violet (MV) is a cationic triphenylmethane dye extensively used in textile dyeing, paper printing, leather processing, paints, inks, and microbiological staining applications [8]. Methyl violet is highly visible even at low concentrations and is difficult to remove by conventional biological treatment methods because of its high solubility and stable aromatic structure[7].

Various treatment technologies have been investigated which include coagulation-flocculation, membrane filtration, ion exchange, biological treatment, electrochemical oxidation, photocatalytic degradation, advanced oxidation processes, ozonation, solvent extraction, and adsorption[1],[2],[9]. Although many of these methods are effective under specific conditions, they often suffer from limitations such as high operating costs, sludge generation, membrane fouling, incomplete pollutant removal, and secondary pollution[7],[8].

Among the available technologies, adsorption has emerged as one of the most promising methods for wastewater treatment which offers advantages such as ease of operation, low energy requirements, economic feasibility, and applicability to a wide range of pollutants[9].

The effectiveness of adsorption largely depends on the nature of the adsorbent employed. Activated carbon has traditionally been considered the most effective adsorbent due to its high surface area and adsorption capacity[10]. However, its relatively high production and regeneration costs have encouraged researchers to investigate alternative low-cost materials[11]. Consequently, a wide range of natural, agricultural, mineral-based, and industrial waste adsorbents have been explored for methyl violet removal.

Various low-cost, natural[12], mineral-based[13], and engineered adsorbents[14] have been investigated for the removal of methyl

violet from aqueous solutions. These studies demonstrate the potential of low-cost adsorbents for dye removal; however, the application of soda feldspar for methyl violet adsorption remains largely unexplored.

Aluminosilicate minerals are particularly attractive because of their availability, structural stability, ion-exchange properties, and surface activity. Soda feldspar, a naturally occurring aluminosilicate mineral, possesses these desirable characteristics and therefore represents a promising adsorbent for wastewater treatment.

Therefore, the present study focused on the potential of soda feldspar as a natural adsorbent for the removal of methyl violet dye from aqueous solutions. The effects of contact time, solution pH, and adsorbent dosage were investigated. Adsorption kinetics and equilibrium behavior were also evaluated. In addition, thermodynamic parameters were also determined to better understand the adsorption mechanism and feasibility of the process.

2. MATERIALS AND METHODS

2.1. Materials: Methyl Violet ($C_{23}H_{26}N_3Cl$) a triphenylmethane dye (molecular weight = 393.96) was procured from M/s Qualigens. Powdered Soda Feldspar (NF) is a naturally available material was procured from Andhra Pradesh, India. The powdered particles were sieved, and particles of size -140 mesh +170 mesh were collected, with an average size of 96.5 μm used in all the experimental studies. All reagents used in this investigation were of A.R. grade. Double distilled water was used for preparing solutions throughout the study.

All pH measurements were carried out with a digital pH meter model number WTH-10, M/s Wensar, India. Concentration of the dye solutions were estimated using absorbance recorded on UV/VIS spectrophotometer model number CE7400 (M/s Cecil, England) over the wavelength of 587 nm. The phase analysis studies were conducted on a Rigaku X-ray diffractometer (Japan) in the scan range (2θ) of

20°-80°. The morphological features were examined by using scanning electron microscopy (SEM, JEOL 6480LV, Japan). The zeta potential (ζ) values were measured with the use of zeta sizer (ZS 90, Malvern, UK).

2.2. Methods

2.2.1. Adsorption studies: Experimental studies were mainly carried out by batch technique to obtain rate and equilibrium data. The experiments were performed to observe the effect of pH (range of pH 2 – pH 9), amount of adsorbent (2 g/L – 20 g/L), and contact time (0 – 210 minutes) at known sample concentrations by fixing the temperature, particle size and agitation speed constant. A known amount of adsorbent was taken in 250mL volumetric flasks containing 50mL each of MV adsorbate solution of known concentration. These flasks were then shaken intermittently to attain equilibrium condition of adsorption. The solution obtained was then centrifuged and analyzed spectrophotometrically by measuring the absorbance at λ_{max} of 587 nm.

The extent of adsorption was quantified in terms of percentage removal and adsorption capacity using the following equations (1) and (2).

$$\text{Percentage removal}(\%) = \frac{(C_o - C_t)}{C_o} \times 100 \dots(1)$$

$$q_t = \frac{(C_o - C_t)V}{W} \dots(2)$$

Duplicate experiments were carried out for all the operating variables studied, and only the average values were considered. The average deviation of duplicate results in the concentration units varied within $\pm 1\%$.

2.2.2. Adsorption kinetics: Two kinetic models were tested in these studies. First one is Pseudo-first order model which assumes adsorption rate

is proportional to the number of vacant sites and generally associated with physical adsorption[4]. Another one is Pseudo-second order model assumes proportional to the square of available sites and frequently associated with chemisorption[4]. Their linear forms are given in the equations (3) and (4).

$$\ln(q_e - q_t) = \ln(q_e) - K_1 t \dots(3)$$

$$\frac{t}{q_t} = \frac{1}{K_2 q_e^2} + \frac{1}{q_e} t \dots(4)$$

K_1 is the rate constant for pseudo-first-order adsorption in $(\text{min})^{-1}$ which is obtained from the linear plot of $\ln(q_e - q_t)$ vs t . K_2 is the rate constant for the pseudo-second-order kinetic model obtained graphically from the plot $\frac{t}{q_t}$ vs t .

2.2.3. Equilibrium studies: The adsorption equilibrium studies were carried out at a constant temperature, dosage, and solution pH but with variable concentrations. Using experimental data, Isotherm models were developed to describe the distribution of dye between the solid phase and the solution when the equilibrium was attained at a given temperature[15]. Five isotherm models, namely Langmuir, Freundlich, Temkin, Dubinin-Radushkevich, and Redlich-Peterson, were employed in this work to study the adsorption mechanism. All the equilibrium models relating the amount of dye adsorbed at equilibrium (mg/g) and the concentration at equilibrium (mg/L) are summarized in the Table.1

2.2.4. Thermodynamics

Thermodynamic analysis helps evaluate the feasibility and nature of the adsorption process. The change in enthalpy ΔH^0 and entropy ΔS^0 of adsorption can be determined using van't Hoff equation (15)

TABLE. 1. EQUILIBRIUM ISOTHERM MODELS EMPLOYED IN ADSORPTION STUDIES

Model	Equation	Linear form	Significance
Langmuir[16]	$q_e = \frac{K_L q_m C_e}{1 + q_m C_e} \dots (5)$	$\frac{C_e}{q_e} = \frac{C_e}{q_m} + \frac{1}{K_L q_m} \dots (6)$	Monolayer adsorption on homogeneous surface; No molecular interactions
Fruendlich[17]	$q_e = K_F C_e^{1/n} \dots (7)$	$\ln q_e = \ln K_F + \frac{1}{n} \ln C_e \dots (8)$	Empirical model; multilayer adsorption on heterogeneous surfaces.
Redlich–Peterson[18]	$q_e = \frac{K_R C_e}{1 + \alpha C_e^\beta} \dots (9)$	$\ln \left(K_R \frac{C_e}{q_e} - 1 \right) = \ln \alpha + \beta \ln (C_e) \dots (10)$	Hybrid isotherm; combining features of Langmuir and Freundlich models.
Dubinin–Radushkevich (D–R)[19]	$q_e = q_s \exp(-K_{DR} \varepsilon^2)$ $\varepsilon = RT \ln \left(1 + \frac{1}{C_e} \right) \dots (11)$	$\ln q_e = \ln q_s - K_{DR} \varepsilon^2 \dots (12)$	estimate adsorption energy ; distinguish physical from chemical adsorption.
Temkin[20]	$q_e = \frac{RT}{b_T} \ln (K_T C_e) \dots (13)$	$q_e = B (\ln K_T) + B (\ln C_e) \dots (14)$	adsorbent–adsorbate interactions; heat of adsorption decreases linearly with surface coverage.

$$\Delta G^0 = \Delta H^0 - T \Delta S^0 \dots (15)$$

Where the gibbs free energy is evaluated using the equation (16) as a function of Langmuir constant at a given temperature [21]

$$\Delta G^0 = -RT \ln(K_L) \dots (16)$$

3. RESULTS AND DISCUSSION

3.1. Characterization of Adsorbent material

The morphological features of the NF sample before and after adsorption of MV dye were examined from SEM images as shown in Fig. 2. Before adsorption, the NF sample (cf. Fig. 2a) exhibited a coarse grained microstructure with random distribution of tabular feldspar particles having a size range of 1-5 μm. These tabular feldspar particles possess irregular layered structure with rough surface morphology. The distribution of interstitial pores indicates the existence of moderate porosity in NF sample. However, it is well known that the rough surface morphology and porous structure provides more adsorptive sites for dye adsorption. After adsorption, SEM image of the NF-MV sample (cf. Fig. 2b) has shown the trapping of MV dye particles onto the cleavage portions of the feldspar particle surface as well as their adsorption into the interstitial pores, which is

The physio-chemical characteristics of the soda feldspar (NF) sample before and after adsorption of the methyl violet (MV) dye were evaluated. X-ray diffraction (XRD) pattern of the soda feldspar (NF) sample before adsorption is presented in Fig. 1. Here the phase analysis of NF sample showed the coexistence of Na, K, Al, and Si bearing minerals, namely quartz (Q; JCPDS card no. 46-1045), microcline (M; JCPDS card no. 19-0932), and albite (A; JCPDS card no. 09-0466) indicating that the dye adsorption mechanism of the NF-MV sample contains pore filling.

The Zeta potential (ζ) values of NF samples before and after adsorption of MV dye are plotted in Fig. 3. It is seen that the ζ value of NF sample before adsorption was -27.6 mV, indicating the negative surface charge of feldspar particles. The ζ value of NF-MV sample was reduced to -25.8 mV after adsorption of the MV dye. This causes a net change in the ζ value of +1.8 mV, showing MV as a positively charged cationic dye. A careful analysis of this data explains that the adsorption mechanism of soda feldspar involves electrostatic force of attraction at dye/adsorbent interface, which leads to adsorption of considerable amount of MV dye molecules onto the negatively charged surface of coarse-grained feldspar particles in NF-MV sample (cf. Fig. 2b).

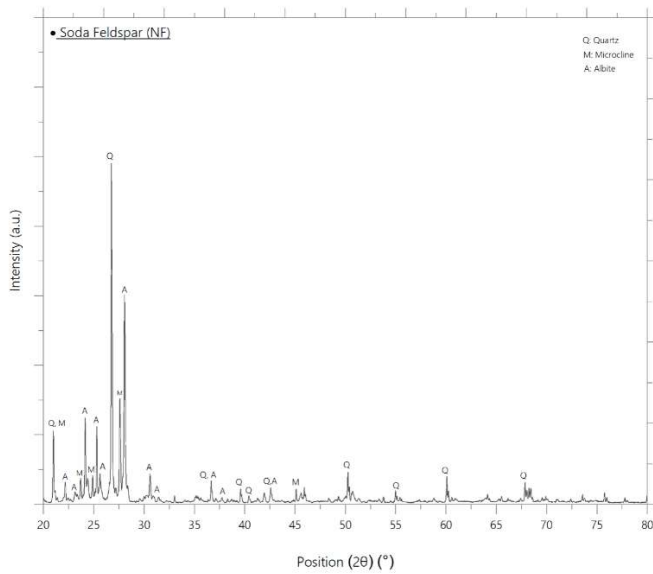


Fig. 1: X-ray diffraction spectra of the soda feldspar (NF) sample

3.2. Effect of contact time

The contact time for adsorption of MV dye onto NF was tested at two different initial concentrations (10 mg/L and 20 mg/L) indicated in Fig. 4. As shown in the graph, the dye removal was very high in the first 5 minutes and after that, increment was slow. The maximum removal was observed at 90 minutes and any further increase in removal was not noted. The higher initial rate of removal was due to the greater surface area on the adsorbent available for active site adsorption. As dye molecules occupied more sites, the adsorbent became saturated and eventually reached equilibrium at 90 minutes. The same pattern was observed at both initial concentrations.

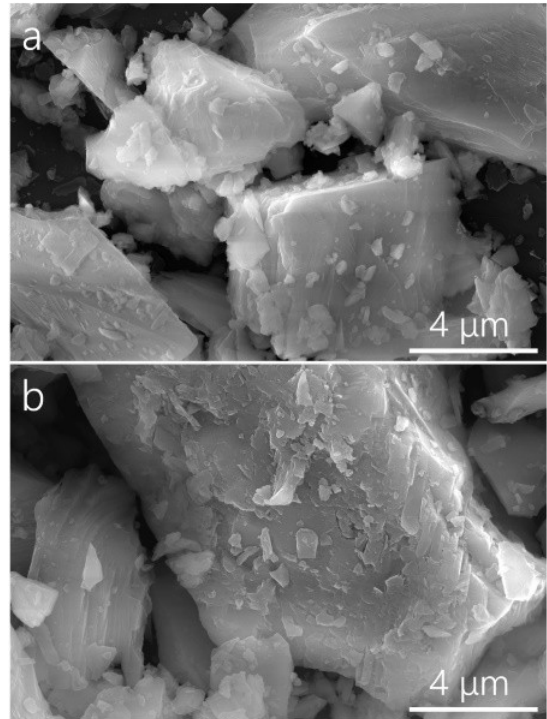


Fig. 2: Scanning electron microscopy (SEM) of (a) NF and (b) NF-MV samples

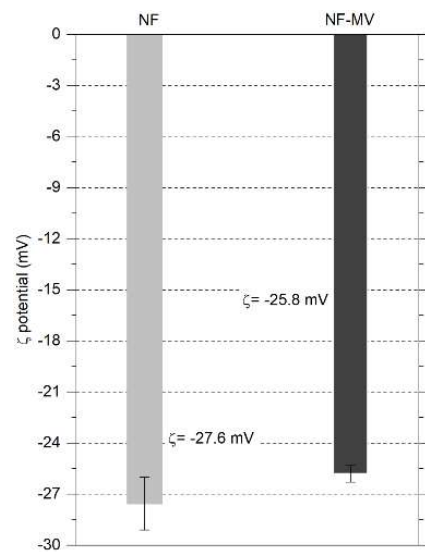


Fig. 3: ζ potential of NF and NF-MV samples

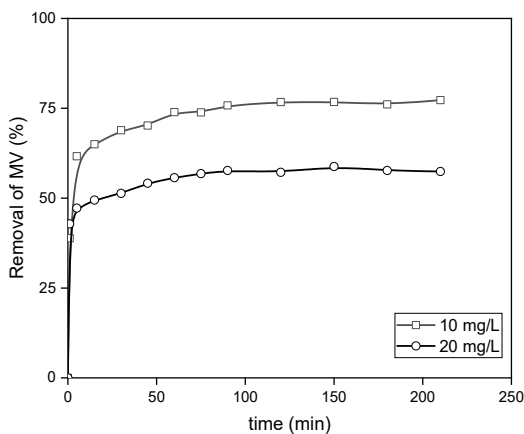


Fig. 4: Effect of contact time

3.3. Effect of pH

Since the surface charge of the mineral can affect the adsorption behavior, it is usual for pH to have an impact on the adsorption of dyes on minerals. It can be seen from the experimental data presented in Fig. 5. that the adsorption of MV dye onto NF was greatly influenced by pH of the solution, as the best removal was seen in the pH of 7–9.

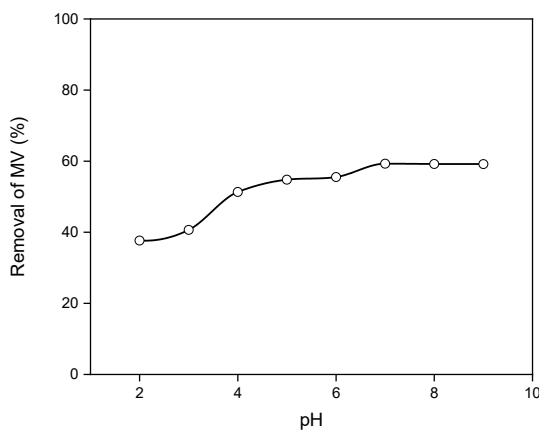


Fig. 5: Effect of pH

The optimal removal of the dye was achieved at pH 7, suggesting that the surface charge of NF possessed at this pH was most compatible with the dye to adsorb onto it. The NF surface may have acquired a positive charge at pH values below 7, potentially resulting in

electrostatic repulsion between the positively charged surface and the positively charged MV dye molecules, hence decreasing adsorption. Similarly, the surface of NF may have acquired a negative charge at pH levels exceeding 7 which induced the attraction between the surface and MV dye molecules, enhancing adsorption.

3.4. Effect of adsorbent dosage

The effect of adsorbent dosage for the removal of MV dye was presented in the Fig. 6 in the range of 2 g/L to 30 g/L. It shows that with the increase of adsorbent dosage up to 20 g/L, the removal of MV dye increased up to 95.4 percent as the higher amount of adsorbent material leading to greater adsorption capacity. More adsorbent implies greater quantity of dye molecules can be sequestered from the solution. This phenomenon is due to the enlarged surface area provided by the additional adsorbent, which can offer more active sites for the dye molecules to adsorb. There is no significant increase in

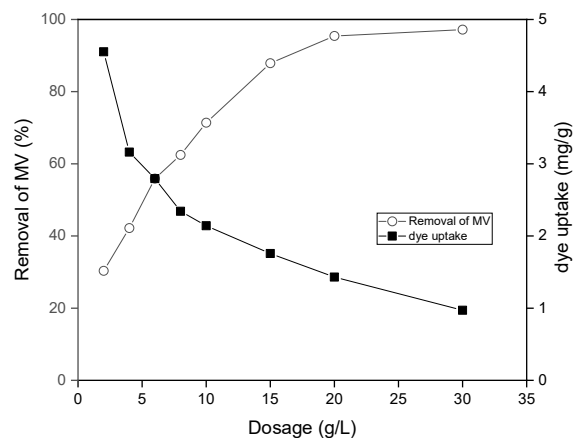


Fig. 6: Effect of adsorbent dosage

percentage removal with increase in adsorbent dosage beyond 20 mg/L. This happens when all adsorption sites on the surface of the adsorbent material have been utilized and are filled with the dye molecules. At this saturation limit, adding more adsorbent does not enhance dye adsorption or substantially elevate the removal percentage. The adsorbent dosage was set at 20 g/L to achieve maximum removal of MV and enhance

economic efficiency for a given initial concentration of 30 mg/L. There was little variation in removal effectiveness, confirming that higher dosages were not beneficial.

3.5. Adsorption kinetics

Two kinetic models were employed, namely the pseudo-first order and pseudo-second-order models, to fit the experimental data and the corresponding graphs are displayed in Fig. 7 and Fig. 8. The parameters obtained from the graphs were compiled in Table. 2.

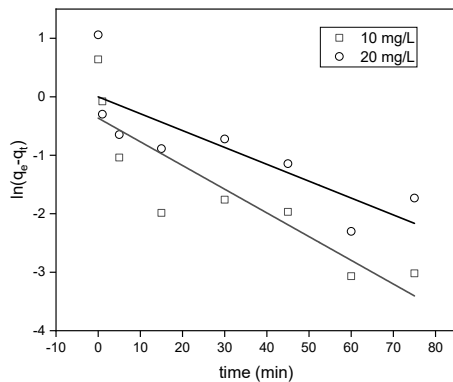


Fig. 7: Pseudo-first order model for the adsorption of MV using NF

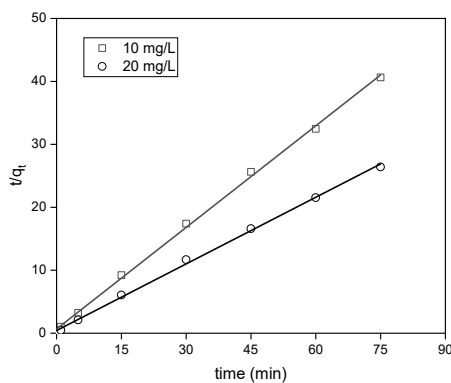


Fig. 8: Pseudo-second order model for the adsorption of MV using NF

Based on the tabulated parameters and the correlation coefficients, the pseudo-second-order model is the most suitable model for describing this study's kinetics of the adsorption process.

TABLE. 2: KINETIC PARAMETERS FOR THE ADSORPTION OF MV USING NF

Parameter	Value	
Initial MV Concentration (mg/L)	10	20
Experimental q_e value (mg/g)	1.89	2.88
Pseudo-first order		
Rate constant (K_1)	0.04	0.04
Calculated q_e value (mg/g)	0.79	1.07
Correlation coefficient (R^2)	0.86	0.87
Pseudo-second order		
Rate constant (K_2), (g/mg.min)	0.43	0.29
Calculated q_e value (mg/g)	1.85	2.83
Correlation coefficient (R^2)	0.99	0.99

3.6. Adsorption isotherms

In order to determine the appropriate adsorption isotherm for the adsorption of MV dye on NF, data was collected and analyzed using various isotherm models such as Langmuir, Freundlich, Temkin, Dubinin-Radushkevich, and Redlich-Peterson isotherm. The parameters obtained from the linear fitting of the experimental data to these models were compiled in Table.3.

A comparison plot of all isotherm models tested was created and shown in Fig. 9. This plot allowed for a visual assessment of the performance and agreement of the different isotherm models in capturing the adsorption behavior of MV dye on NF.

Overall, the analysis indicated that the Langmuir and Redlich-Peterson isotherm models were suitable for describing the adsorption process, with the best fit to the experimental data. This suggests that MV molecules are adsorbed on the homogenous surface of the NF in monolayer fashion without molecular interactions. This information provides valuable insights into the adsorption mechanism and can assist in optimizing the design and operation of adsorption systems for removing MV dye using NF.

TABLE 3: VARIOUS ISOTHERM PARAMETERS FOR THE ADSORPTION OF MV USING NF

Isotherm model	Parameters	Units	Value	R ²	Remarks
Langmuir	q _m	mg/g	3.90	0.99	best fit
	K _L	L/mg	0.35		
Freundlich	K _F	(mg/g)/(mg/L) ^(1/n)	2.04	0.98	best fit
	N	-	6.59		
Temkin	K _T	L/mg	82.76	0.98	best fit
	b _T	J/mol	5743.79		
Dubinin-Radushkevich	K _{DR}	L/mg	3.07E-06	0.81	good fit
	q _s	mg/g	3.47		
Redlich-Peterson	K _R	L/mg	2.8	0.99	best fit
	β	-	0.73		
	α	(L/mg) ^β	1.01		

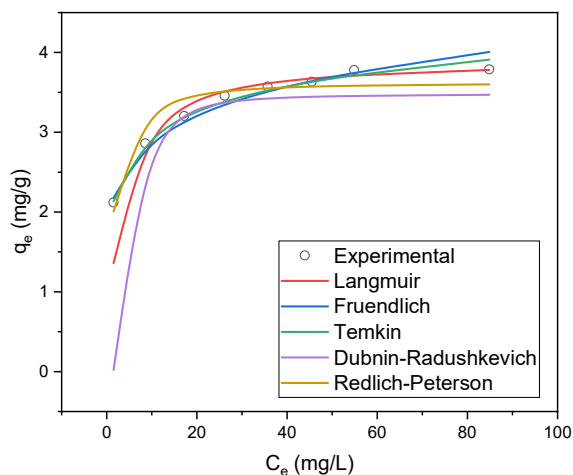


Fig. 9: Comparison of various adsorption isotherms

3.7. Adsorption thermodynamics

Using the equilibrium data collected at three different temperatures, 313K, 323K and 333K, ΔG , ΔH and ΔS were calculated with other thermodynamic parameters using the Langmuir constant with Gibbs' equation. The computed values are included in Table. 4.

In Fig. 10, it is clear that the Gibbs function free energy yields lower negative values with increasing temperature, which means that higher temperatures are more beneficial. Furthermore, the increase in enthalpy supports the reason for the observed endothermic process. The process is also found to be irreversible, as indicated by the increase in entropy

TABLE 4: THERMODYNAMIC PARAMETERS FOR THE ADSORPTION OF MV USING NF

Temperature (K)	Langmuir Constant, K _L (-)	ΔG (kJ/mol.K)	ΔH (kJ/mol)	ΔS (J/mol.K)
313	0.966	-33.44	11.521	143
323	1.004	-34.61		
333	1.258	-36.31		

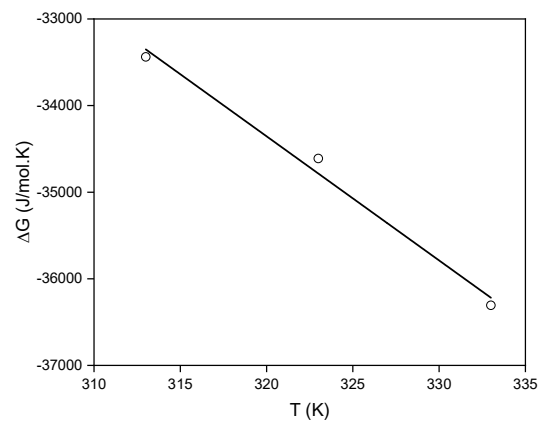


Fig. 10: Gibbs free energy change with temperature

4. CONCLUSION

Batch adsorption experiments showed that the process was influenced by contact time, pH, initial dye concentration, adsorbent dosage, and temperature, with a maximum dye removal efficiency of 95.4% achieved under optimized conditions. The favourable adsorption performance observed at near-neutral pH highlights the practical applicability of soda feldspar for wastewater treatment.

Kinetic analysis revealed that adsorption was primarily governed by interactions between methyl violet molecules and the active sites present on the soda feldspar surface. Equilibrium

data were best described by the Langmuir isotherm model, indicating predominantly monolayer adsorption on a relatively homogeneous surface.

Thermodynamic parameters confirmed that the adsorption process was spontaneous and endothermic in nature. The adsorption mechanism is likely governed by a combination of electrostatic attraction, surface complexation, and weak intermolecular interactions between the cationic dye molecules and the aluminosilicate surface of soda feldspar. Overall, the results indicate that soda feldspar is an environmentally friendly and economically viable adsorbent for the treatment of dye-contaminated wastewater.

NOMENCLATURE

Symbol	Abbreviation	Units
b_T	Temkin constant	J/mol
C_e	Equilibrium concentration of adsorbate solution	mg/L
C_o	Initial concentration of adsorbate solution	mg/L
C_t	Concentration of adsorbate solution at any time	mg/L
E	Adsorption energy	kJ/mol
ΔG	Change in Gibbs free energy	J/kmol
ΔH	Change in enthalpy	J/kmol
K_F	Freundlich constant	L/mg
K_L	Langmuir constant	L/mg
K_{DR}	Mean free energy exchange	mol ² /kJ ²
K_T	Temkin isotherm equilibrium binding constant	L/mg
K_R	Redlich-Peterson constant	L/mg
K_1	Pseudo-first-order rate constant	min ⁻¹
K_2	Pseudo-second-order rate constant	(mg/g) ⁻¹ min ⁻¹
n	Freundlich heterogeneity factor	(-)
q_e	Amount of adsorbate per unit mass of adsorbent at equilibrium	mg/g
q_m	Langmuir constant	mg/g
q_t	Amount of adsorbate per unit mass of adsorbent at time t	mg/g
R	Ideal gas constant	J/mol·K
ΔS	Change in entropy	J/kmol
T	Temperature	K
t	Time	min
V	Volume of solution	L
W	Mass of the adsorbent	g
α	Redlich-Peterson constant	(L/mg) ^β
β	Redlich-Peterson exponent	(-)
ε	Polanyi potential	kJ/mol

REFERENCES

- Esra Altıntiğ, Açelya Alsancak, Huseyin Karaca, Dilek Anım and Hüseyin Altundag, "The comparison of natural and magnetically modified zeolites as an adsorbent in methyl violet removal from aqueous solutions", *Chemical Engineering Communications*, 209(4), pp. 555-569 (2021). DOI: <https://doi.org/10.1080/00986445.2021.1874368>
- Makfir Sadiku, Teuta Selimi, Avni Berisha, Arsim Maloku, Valbonë Mehmeti, Vepirim Thaçi and Naim Hasani, "Removal of Methyl Violet from Aqueous Solution by Adsorption onto Halloysite Nanoclay: Experiment and Theory", *Toxics* 445(10), (2022). DOI: <https://doi.org/10.3390/toxics10080445>
- H. V. Mehr, J. Saffari, S. Z. Mohammadi and S. Shojaei, "The removal of methyl violet 2B dye using palm kernel activated carbon: thermodynamic and kinetics model", *International Journal of Environmental Science and Technology*, 17, pp. 1773-1782 (2020). DOI: <https://doi.org/10.1007/s13762-019-02271-0>
- Manel Wakkal, Besma Khiari and Féthi Zagrouba, "Basic red 2 and methyl violet adsorption by date pits: adsorbent characterization, optimization by RSM and CCD, equilibrium and kinetic studies", *Environmental Science and Pollution Research*, 26, pp. 18942–18960 (2019). DOI: <https://doi.org/10.1007/s11356-018-2192-y>
- Daniel Omeodisemi Omokpariola and Joy Njoku Otuosorochi, "Batch Adsorption Studies on Rice Husk with Methyl Violet Dye", *World News of Natural Sciences*, 33, pp. 48–63 (2020).
- Widi Astuti, Achmad Chafidz, Endang Tri Wahyuni, Agus Prasetya, I Made Bendiyasa and Ahmed E. Abasaed, "Methyl Violet Dye Removal using Coal Fly Ash (CFA) as a Dual Sites Adsorbent", *Journal of Environmental Chemical Engineering*, 7(5), 103262 (2019). DOI: <https://doi.org/10.1016/j.jece.2019.103262>
- Eunae Cho, Muhammad Nazir Tahir, Hwanhee Kim, Jae-Hyuk Yu and Seunho Jung, "Removal of methyl violet dye by adsorption onto N-benzyltriazole derivatized dextran", *RSC Advances*, 43, (2015). DOI: <https://doi.org/10.1039/C5RA03317A>
- H. Mittal, Vaneet Kumar, Saruchi and Suprakas Sinha Ray, "Adsorption of methyl violet from aqueous solution using gum xanthan/Fe₃O₄ based nanocomposite hydrogel", *International Journal of Biological Macromolecules*, 89, pp. 1–11 (2016). DOI: <https://doi.org/10.1016/j.ijbiomac.2016.04.050>
- Nisreen S. Ali, Noor M. Jabbar, Saja M. Alardhi, Hasan Sh. Majdi and Talib M. Albatayti, "Adsorption of methyl violet dye onto a prepared bio-adsorbent from date seeds: isotherm, kinetics, and thermodynamic studies", *Heliyon*, 8(8), e10276 (2022). DOI: <https://doi.org/10.1016/j.heliyon.2022.e10276>
- Yohan Kim, Jiyeol Bae, Hosik Park, Jeong-Kwon Suh, Young-Woo You and Heechul Choi, "Adsorption dynamics of methyl violet onto granulated mesoporous carbon: Facile synthesis and adsorption kinetics", *Water Research*, 101(5), pp. 187–194 (2016). DOI: <https://doi.org/10.1016/j.watres.2016.04.077>
- Haoying Zhai, Jinshan Zou, Fuming Liu, Fangyuan Chen, Xingrong Yan and Wen-Jun Zhou, "Adsorption removal of methyl violet from aqueous solution by chromium phosphovanadate", *Surface and Interface Analysis*, 53(1), pp. 76–83 (2021). DOI: <https://doi.org/10.1002/sia.6874>
- Muhammad Raziq Rahimi Kooch, Muhammad Khairud Dahri, Linda B. L. Lim, Lee Hoon Lim and Owais Ahmed Malik, "Batch adsorption studies of the removal of methyl violet 2B by soya bean waste: isotherm, kinetics and artificial neural network modelling", *Environmental Earth Sciences*, 75, 783 (2016). DOI: <https://doi.org/10.1007/s12665-016-5582-9>
- K.S. Rani, G.V.S. Sarma, K.G. Naidu, K. V Ramesh, Adsorptive removal of chromium by modified laterite, in: *Mater. Today Proc.*, Elsevier Ltd., 18(7), pp. 4882–4892 (2019). DOI: <https://doi.org/10.1016/j.matpr.2019.07.479>
- Suriyan Radha, Paul Christygnanatheeba, Karuppiah Nagaraj, Saradh Prasad, Mohamad Saleh AlSalhi, Jeyaraj Vinoth Kumar, Prabhakarn Arunachalam and Chelladurai Karuppiah, "Titanium(III) Oxide Doped with meta-Aminophenol Formaldehyde Magnetic Microspheres: Enhancing Dye Adsorption toward Methyl Violet", *Processes*, 11(4), 1250 (2023). DOI: <https://doi.org/10.3390/pr11041250>

15. A.M. Aljeboree, A.N. Alshirifi, A.F. Alkaim, "Kinetics and equilibrium study for the adsorption of textile dyes on coconut shell activated carbon," *Arabian Journal of Chemistry*, 10(2), S3381–S3393 (2017). DOI: <https://doi.org/10.1016/j.arabjc.2014.01.020>.
16. J. Zhang, Y. Li, C. Zhang, Y. Jing, "Adsorption of malachite green from aqueous solution onto carbon prepared from *Arundo donax* root," *Journal of Hazardous Materials*, 150(3), 774–782 (2008). DOI: <https://doi.org/10.1016/j.jhazmat.2007.05.036>.
17. A. Sharma, Z.M. Siddiqui, S. Dhar, P. Mehta, D. Pathania, "Adsorptive removal of congo red dye (CR) from aqueous solution by *Cornulaca monacantha* stem and biomass-based activated carbon: isotherm, kinetics and thermodynamics," *Separation Science and Technology*, 54(6), 916–929 (2019). DOI: <https://doi.org/10.1080/01496395.2018.1524908>.
18. Indra D. Mall, Vimal C. Srivastava, Nitin K. Agarwal, "Removal of Orange-G and Methyl Violet dyes by adsorption onto bagasse fly ash—kinetic study and equilibrium isotherm analyses", *Dyes and Pigments*, 69(3), pp. 210-223 (2006). DOI: <https://doi.org/10.1016/j.dyepig.2005.03.013>.
19. M.D.G. de Luna, E.D. Flores, D.A.D. Genuino, C.M. Futralan, M.W. Wan, "Adsorption of Eriochrome Black T (EBT) dye using activated carbon prepared from waste rice hulls-Optimization, isotherm and kinetic studies," *Journal of the Taiwan Institute of Chemical Engineers*, 44(4), pp. 646–653 (2013). DOI: <https://doi.org/10.1016/j.jtice.2013.01.010>.
20. M. Dastkhooon, M. Ghaedi, A. Asfaram, A. Goudarzi, S.M. Langroodi, I. Tyagi, S. Agarwal, V.K. Gupta, "Ultrasound assisted adsorption of malachite green dye onto ZnS:Cu-NP-AC: Equilibrium isotherms and kinetic studies - Response surface optimization," *Separation and Purification Technology*, 156(2), 780–788 (2015). DOI: <https://doi.org/10.1016/j.seppur.2015.11.001>.
21. A.A. Jalil, S. Triwahyono, S.H. Adam, N.D. Rahim, M.A.A. Aziz, N.H.H. Hairom, N.A.M. Razali, M.A.Z. Abidin, M.K.A. Mohamadiah, "Adsorption of methyl orange from aqueous solution onto calcined Lapindo volcanic mud," *Journal of Hazardous Materials*, 181(1-3), pp. 755–762 (2010). DOI: <https://doi.org/10.1016/j.jhazmat.2010.05.078>.